

COMPUTATIONAL MODELING OF POSITRON  
ANNIHILATION IN SOLIDS

by

John Carter Barrett

A senior thesis submitted to the faculty of

Brigham Young University

in partial fulfillment of the requirements for the degree of

Bachelor of Science

Department of Physics and Astronomy

Brigham Young University

March 2013

Copyright © 2013 John Carter Barrett

All Rights Reserved

BRIGHAM YOUNG  
UNIVERSITY

DEPARTMENT  
APPROVAL

of a senior thesis submitted  
by

John Carter Barrett

This thesis has been reviewed by the research advisor, thesis coordinator,  
and Committee Member and has been found to be satisfactory.

---

Date

---

Evan Hansen, Advisor

---

Date

---

Stephen McNeil, Thesis Coordinator

---

Date

---

Stephen Turcotte, Committee Member

## ABSTRACT

### COMPUTATIONAL MODELING OF POSITRON ANNIHILATION IN SOLIDS

John Carter Barrett

Department of Physics and Astronomy

Bachelor of Science

This thesis provides an introduction to computational simulation of positron spectroscopy. The topic is approached by a two part method: first, a study of modern computational methods; and secondly, the juxtaposition of computational and experimental data, to test the accuracy of the computational methods, used. A brief overview of positron spectroscopy provides a needed foundation, and allows for an exposition on the mathematical methods used in computational simulation. Two Component Density Functional Theory is addressed as the principle method, along with useful simplifications; including, the Conventional Scheme, and Atomic Superposition. A case study compares experimental results of positron spectroscopy to corresponding computational results, calculated in house. The MIKA Doppler program, developed at Helsinki University of Technology, is chosen as the main tool for the simulations, because of its accedence by the research community. The simulations each model a copper super-cell—one with a single vacancy, and another with no vacancies. The experimental data was collected through positron spectroscopy on copper samples with varying amounts of vacancy concentrations. The resulting—experimental and computational—energy distributions are compared show significant agreement in the effect of vacancy concentration on line shape parameter. Adversely, small characteristic differences between the compared distributions are identified and discussed. Overall, the collaboration between results in the case study lends credence to the validity of the computational methods discussed and used in this thesis.

## ACKNOWLEDGMENTS

Thank you to the physics department, at Brigham Young University – Idaho, for the positron spectroscopy setup, experimental data, information, and support. Including a specific acknowledgment of Bro. Evan Hansen; who leads the positron spectroscopy research, mentored this thesis, and initiated the project. Lastly, this thesis owes much of its success to the physics department of Helsinki University of Technology; who developed, and made available, the MIKA Doppler program.

# Contents

Table of Contents	vi
List of Figures	vii
List of Tables	iix
<b>1 Introduction</b>	<b>1</b>
1.1 Overview . . . . .	1
1.2 Applications . . . . .	3
1.3 Background: Positron Spectroscopy . . . . .	3
<b>2 Computational Method</b>	<b>7</b>
2.1 General Methods . . . . .	7
2.2 Procedure . . . . .	9
2.3 MIKA Program Outline . . . . .	10
2.4 Data Processing . . . . .	11
<b>3 Copper Simulation</b>	<b>13</b>
3.1 Overview . . . . .	13
3.2 Computational Results . . . . .	14
<b>4 Parity with Experiment</b>	<b>19</b>
4.1 Experimental Method . . . . .	19
4.2 Comparison of Data . . . . .	20
4.3 Discrepancies . . . . .	22
<b>5 Ending</b>	<b>23</b>
 Bibliography	 24
A Appendix: Samples	25

## List of Figures

1.	Diagram of photon emission . . . . .	4
2.	Sample photon energy distribution . . . . .	5
3.	Iso-level plot of electrons in a small copper structure . . . . .	12
4.	Iso-level plot of electrons in a bulk copper super-cell . . . . .	14
5.	Iso-level plot of a positron in a bulk copper super-cell . . . . .	15
6.	Iso-level plot of a positron in a defect-rich copper structure . . . . .	16
7.	Simulated momentum distributions . . . . .	17
8.	Comparison of energy distribution . . . . .	20
9.	S parameters of varying defect densities . . . . .	21

## List of Tables

1.	Step outline of program operations. . . . .	10
2.	Matlab code used to form particle density data . . . . .	11
3.	Simulation line-shape parameters . . . . .	18

# Chapter 1

## Introduction

### 1.1 Overview

Modern physics research is progressively studying smaller structures, thus creating the challenge of observing material properties on an atomic scale. Positron annihilation spectroscopy has developed in response to this need, being used to observe the state of vacancy type defects at the atomic level in materials. More so, the computational modeling of this useful process allows for unique research opportunities: providing a better understanding of the physics of annihilation, and the reliability of positron spectroscopy as a whole.

This thesis covers the general methods of simulating positron spectroscopy, but places a significant focus on the methods applied in this thesis. All documented simulations are performed using an accepted program, MIKA Doppler, written at the Helsinki University of Technology.

Positron spectroscopy simulations utilize Two Component Density Functional Theory(TCDFT), and the Kohn Sham method; to model both, the wave function of the electrons in the solid, and the wave function of thermalized positron. The details of the annihilation events are solved using these wave functions. Important output data from the simulation includes a momentum distribution of annihilations, and the



positron's expected lifetime; both of which can be compared to experimental results.

Two computational simulations of atomic super-cells provide data for this thesis: a bulk(vacancy free) formation of copper, and a copper formation containing a single vacancy. The output data from simulations is transferred from the MIKA program into Matlab, to be processed. The units are converted, and the data is formed in such a way to imitate experimental results collected in lab experiments.

Experimental data on copper is compared to the computational results. The experimental data was collected by the BYU-Idaho physics department, through positron spectroscopy of copper samples, which varying amounts of defects.

A strong correlation between the computational and experimental results is apparent, and strengthens our confidence in the accuracy of the simulations. However, some inconsistencies between experimental and computational data do exist. This inconsistency is mostly attributed to inherent background noise and precision of experimental methods.

Additionally, an important insight is made possible by the computational data. The computational data clearly distinguishes between valence and core annihilation events, due to its noiseless results and ability to calculate annihilation events in isolated electron shells. This shell specific energy distribution can be used to predict energy bounds that correspond strongly to either valence or core events. These bounds provide a method of defining a shape parameter (a value to describe the shape of the energy distribution) that maybe more sensitive to defects than the standard S parameter that is often used.

This thesis concludes that computational simulations of positron spectroscopy provide results that show agreement with its experimental counterparts. This parity between results demonstrates the validity of current scientific theory, and the accuracy of computational methods for modeling positron-electron interactions. The research also opens doors for further investigation of the discrepancies between experimental and computation results, and methods to resolve them.

## 1.2 Applications

Positron annihilation spectroscopy is beneficial because the concentration of defects in a material dramatically effects the material's electronic, mechanical and optical properties. Experimental methods using positron spectroscopy can observe the evolution of defects as a result of time or wear. This information is particularly useful when applied to semi-conductors, resistors, or crystal formations. Positron spectroscopy research is commonly used to study the effect of heat on the defect concentrations in semi-conductors and metals. It is also used to observe the evolution of metal structures due to oxidation. Even in the biological setting, the method is used in imaging as part of sPEC and PET scans.[1]

Developing a computational model of the processes occurring during Positron Spectroscopy, or annihilation in solids in general, is also valuable. Producing such a model tests the accuracy of current scientific theories in the area. If a computational model is built using accurate theories, the results should agree with real world observation. Thus in positron annihilation, the agreement between analogous experimental and computational data, generates greater confidence in the theories applied in the computational model. These theories are wide ranging, relating to annihilation , Doppler energy broadening, and quantum mechanics. Simulations are also important because they allow deeper research, and understanding. For instance, knowing how the concentration or shape of defects will influence spectroscopy results, allows positron spectroscopy to be even more informative and accurate. And a better understanding of defect formations and a reliable way to observe them, can provide insight into the evolution of defects and the material properties they cause.

## 1.3 Background: Positron Spectroscopy

Positron Annihilation spectroscopy is often called Doppler broadening spectroscopy, because it measures the Doppler effect in photons emitted during annihilation. Upon entering a solid, an incident positron will quickly thermalize to a

relatively low speed, in thermal equilibrium with the solid. The forces caused by the positively charged nucleons and negatively charged electrons will influence the positron, until it interacts with an electron and annihilates. In the case where the net momentum of both particles is zero, the annihilation will emit two photons in exactly opposite directions, with energies of .511 MeV—which is the rest mass of an electron/positron. However, if the net momentum of the pair is not zero, then the angle between the two emitted photons will differ from 180 degrees by  $\theta$ , given by

$$\sin(\theta) \approx \frac{p_{\perp}}{m_0 c} \quad (1)$$

where  $P_{\perp}$  is the perpendicular component of momentum. Since the kinetic energy of the positron after thermalization, is small compared to that of the electron; the net momentum depends mostly on the electron. Figure 1 depicts how the momentum of the original electron might deflect the emitted photons:

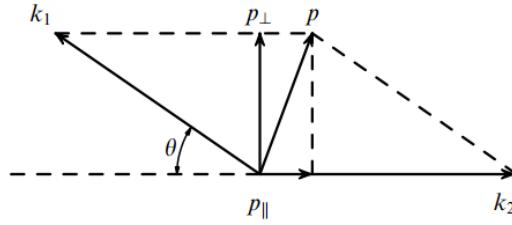


Fig 1: Diagram of photon emission( $k_1$   $k_2$ ) deflected by orthogonal momentum.[1]

And more importantly, the energy of the photons will differ from .511 MeV by  $\Delta E$ ,

$$\Delta E \approx \frac{p_{\parallel} c}{2} \quad (2)$$

where  $P_{\parallel}$  is the parallel momentum. One photon will gain the energy while the other will lose the same energy. This effect is referred to as a Doppler effect, because a photon moving with the parallel momentum will gain the energy, meaning a higher frequency, while a photon moving against this momentum loses energy, meaning a lower frequency.[1]

Using sensors to measure either the energy of emitted photons, or the angle of

deflection between them, one can identify the momentum of the annihilated electron. This information is valuable because low momentum electron annihilation events are correlated to the defect density of a material. Valence electrons have lower kinetic energy than core electrons. When a positron thermalizes near a vacancy, it is attracted to the vacancy's low potential; and there it will likely annihilate with a valence electron from one of the surrounding atoms. If there are few or no vacancies in the atomic structure, the positron is more likely to annihilate with a core electron than if vacancies were present .

Doppler spectroscopy uses a positron source to create many annihilation events in a sample. The emitted photon energies are measured by at least one sensor, but a second sensor can reduce background noise through coincidence detection. The energy distribution of recorded photons will spike around .511 MeV. The parallel momentum distribution of the positron-electron pairs is directly related to the recorded photon energy distribution. More low momentum annihilations with valence electrons will create a sharper spike. And more core annihilations will create a wider spike around the .511 MeV mark. An example of an energy distribution is shown in figure 2:

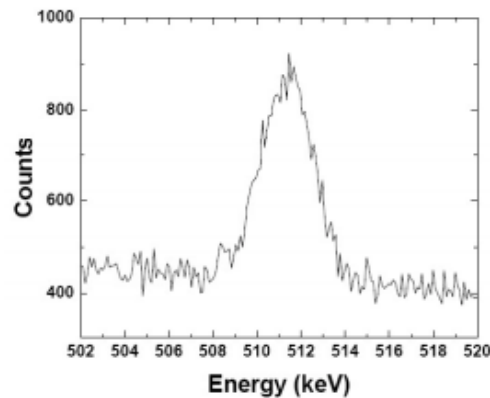


*Fig 2: Sample photon energy distribution[1]*

The sharpness of the distribution curve is described by a line shape parameter  $S$ . The  $S$  parameter measures the portion of counts within a certain width of the peak to the total counts of the peak; thus describing the portion of positron-electron annihilation events that are low energy. As long as the energy bounds of the  $S$  parameter kept consistent among trials, multiple energy distributions can be compared to each other. A standard method of choosing  $S$  parameter energy bounds is to choose the bounds that give a .5 ratio of lower energy to higher energy events, when applied to a pure sample(no defects) of the solid.

# Chapter 2

## Computational Method

### 2.1 General Methods

In order to find the positron and electron densities, two-component density functional theory(TCDFT) is used. TCDFT provides a reasonable calculation method, while still providing sufficient accuracy. Density functional theory models a collection of interacting particles—such as a collection of electrons—as a single non-interacting particle gas with a new effective potential. The effective potential includes the the typical external potentials(coulomb forces etc.) as well as an added potential, that accounts for the ignored interactions between the individual particles.[2] A two component DFT method models both the electron wave function and the positron wave function, as well as the effective potentials for each. These wave functions are often called Kohn-Sham equations, with the process of solving the equations being a Kohn-Sham method. An example of the Kohn-Sham wave equations—which are Schrodinger equations with an adjusted potential,  $V_{\text{eff}}$ —used in the theory are included on the next page,

$$-\frac{1}{2}\nabla^2\psi_i^+(\mathbf{r}) + V_{eff}(\mathbf{r})\psi_i^+ = \varepsilon_i\psi_i^+(\mathbf{r}) \quad (3)$$

$$V_{eff}(\mathbf{r}) = \phi(\mathbf{r}) + \frac{\delta E_{xc}[n_+]}{\delta n_+(\mathbf{r})} + \frac{\delta E_c^{e-p}[n_+, n_-]}{\delta n_+(\mathbf{r})} \quad (4)$$

$$\phi(\mathbf{r}) = \int d\mathbf{r}' \frac{-n_-(\mathbf{r}') + n_+(\mathbf{r}') + n_0(\mathbf{r}')}{|\mathbf{r} - \mathbf{r}'|} \quad (5)$$

where  $n_{+/-0}$  accounts for the positron, electron, and nucleon interactions, respectively.

For the greatest accuracy, the two Schrodinger equations—one for the positron and one for all the electrons—should be solved simultaneously in an iterative method. The MIKA program, however, combines two useful approximations to reduce the amount of calculation required: atomic superposition and the conventional scheme. Atomic superposition superimposes stored free atom potentials and densities, to quickly construct the starting coulomb potential and electron density. The conventional scheme simplifies the TCDFT method, and calculates the final electron density independently of the positron equation. This greatly simplifies the wave function calculations. Combined with an enhancement factor, the conventional scheme still produces results that are acceptably close to a true TCDFT method[3].

The MIKA program performs the Kohn-Sham calculations in an iterative method that calculates points on a coarse grid, and then progressively finer grids. This method is called the Rayleigh quotient multigrid method(RQMG), and it provides accuracy at a low calculation cost.

With both the particle wave functions available, MIKA calculates the annihilation rate for each electron state. The annihilation rates describe the rate at which the positron is likely to annihilate with an electron of that shell.

In this case the annihilation rate is found for each electron state; and it is found by the overlap integral of the electron state wave function and positron wave function:

$$\lambda_j = \pi r_0^2 c \int d\mathbf{r} \gamma^{LDA,GGA}(\mathbf{r}) |\psi_+(\mathbf{r})|^2 |\psi_j(\mathbf{r})|^2 \quad (6)$$

where  $\gamma$  is the enhancement factor,  $r_0$  is the radius of an electron, and  $j$  indicates the state.

Using the state annihilation rates, the program calculates the parallel momentum distribution of annihilating pairs, for each electron state using the following formula:

$$\rho_j(\mathbf{p}) = \pi r_e^2 c u_j^2(0) \left| \int d\mathbf{r} e^{-i\mathbf{p} \cdot \mathbf{r}} \psi_+(\mathbf{r}) \psi_j(\mathbf{r}) \right|^2 \quad (7)$$

Where the  $u_j$  term— $j$  being the electron state—is a state-specific factor, that is calculated from the state-specific annihilation rate. Summing over all electron states provides the final momentum distribution for the positron-electron annihilation pairs[3].

## 2.2 Procedure

This thesis primarily uses the MIKA Doppler program to perform simulations, and processes the resulting data in Matlab. An input file specifies an atomic structure to be simulated. The structure is accurate to atomic structures observed in actual solids of the chosen type; and a specific defect density is applied to the structure, imitating the possible conditions of a physical sample. The MIKA program uses the input file to calculate the Kohn-Sham equations for the electrons and positron, the annihilation rates for each electron shell, and the parallel momentum distribution of the annihilating pairs. Summing over the resulting series of state specific momentum distributions creates a complete momentum distribution. This thesis inputs both the total momentum distribution, and its decomposed form, into matlab. In Matlab, a function converts the parallel momentum of the distribution to Doppler-shifted, photon energies, that would be created and detected in a lab experiment. This thesis also inputs the positron and electron DFT functions into Matlab, and plots them as three dimensional iso-level plots.



## 2.3 MIKA Program Outline

This section specifically delineates the steps taken by the MIKA program to construct a given atomic model, and calculate its resulting momentum distribution. The steps performed in the MIKA program are the most instrumental in simulating Doppler spectroscopy; thus, a complete examination of the program's functions demonstrates the application of computational methods, and justifies the data produced in this thesis.

First, the program reads an input file, that indicates the element, and the three dimensional location of each atom. Then an atomic superposition method superimposes stored potentials and electron densities at the specified locations. Following that, the program models the electron density as a single wave function according to Density Functional Theory. The program then uses a Rayleigh Quotient MultiGrid method to solve the positron Khon-Sham equation, according to DFT, at specific points. According to RQMG, the grid size adjusts until a given resolution is reached. The final electron and positron densities at each grid point are output for plotting. Using the final TCDFT Schrodinger equations, MIKA calculates the annihilation rate for each electron state; which allows for the calculation of the momentum distribution for each said state. The distributions are output as a decomposed version(series of state-specific distributions) and a summed version.

An outline of the steps is provided in table 1 for clarity:

*Table 1: Step outline of MIKA program operations*

- |  |
|--|
| <ul style="list-style-type: none"><li>• Read input file</li><li>• Construct potentials and electron density through atomic superposition of stored values</li><li>• Solve electron wave function and densities</li><li>• Solve positron wave function and densities using RQMG</li><li>• Output electron and positron densities</li><li>• Calculate annihilation rates for electron states</li><li>• Calculate momentum distributions for electron states</li><li>• Output momentum distribution</li></ul> |
|--|

## 2.4 Data Processing

After the data produced by the MIKA program is output, it transfers to Matlab to be further processed. The final positron and electron wave densities are converted to three-dimensional iso-level plots. And the momentum distribution is converted to a photon energy distribution, that would be observed in an actual spectroscopy experiment.

Three-dimensional iso-level plots use colored surfaces to indicate points of equal value, similar to the way a contour plot uses lines in two dimensions . Using partially transparent surfaces, iso-levels can create visually informative plots of particle density “clouds”, that would be otherwise difficult to represent visually. Before the plots can be created, the particle density data must be formatted in a three-dimensional array. The MIKA program exports the particle densities as a single column of values, without any other indicators. The pattern that MIKA exports its data in is a three tiered loop. The values for each point list starting with the points where  $y=1, z=1$ , and listing all the  $x$  coordinates(1-max). Then each  $x$  coordinate where  $y=2, z=1$ , is listed; and so on. This thesis places the data from simulations into a three dimensional matrix, in Matlab, using loops. An example of the process used on a  $56 \times 56 \times 56$  grid size is included in table 2 below.

*Table 2: Matlab code used to form particle density data into 3d matrix.*

```
filename= 'WAVE3d3';
A=importdata(filename);
n=6;
for z = 1:56
    for y = 1:56
        for x = 1:56
            n=n+1;
            W(x,y,z)=A(n);
        end
    end
end
```

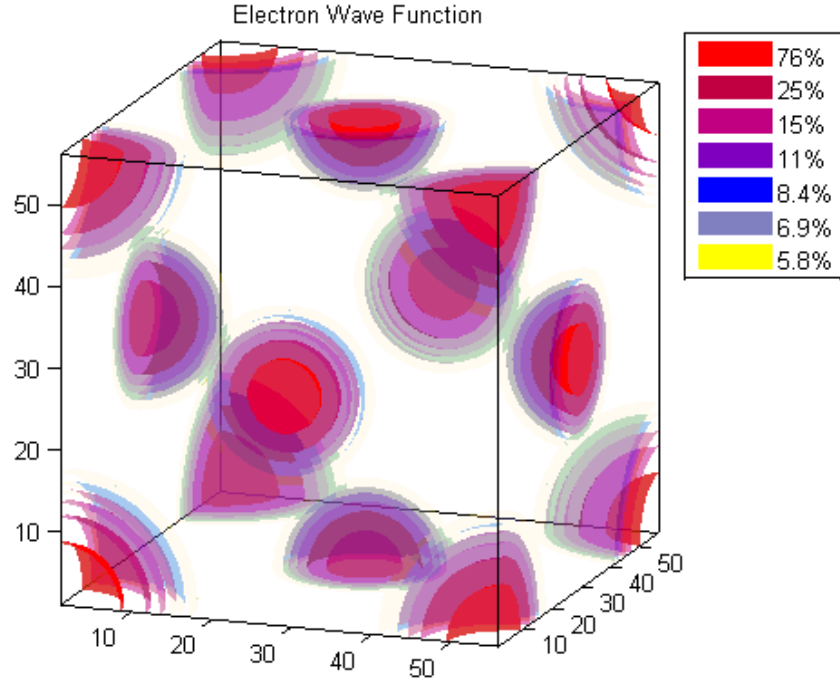


*Fig 3: Electron density of a small copper structure. Iso-levels are labeled as percentages of the highest density point plotted.*

A matlab function uses the three-dimensional array, to plot multiple partially transparent iso-levels. The density value used for each iso-level is set to a percentage of the highest density value found in the array. Figure 3 is an example of an iso-level plot of electron density in a small copper atomic structure.

The MIKA program outputs the momentum distribution of the annihilation pairs in two columns. One column indicates the parallel momentum, and the other indicates the predicted counts. The parallel momentum is given in units of  $10^{-3}m_0c$ , where  $m_0$  is the rest mass of an electron/positron. Using equation (2) we find that 3.91 of these momentum units corresponds to a 1 KeV change in photon energy. Converting the units and centering on .511 MeV creates the Doppler shifted energy spectrum, that the momentum distribution would create.

# Chapter 3

## Copper Simulation

### 3.1 Simulation Overview

Copper is an advantageous material to use in a case study. Both the material and experimental data is available, making it easy to compare to experimental results. It can also be manipulated to introduce, or remove, defects; allowing for comparison against experimental data of both pure and defected samples. More so, copper metal has a well understood atomic structure, that is necessary to construct the computational model.

This thesis simulates positron annihilation spectroscopy for a pure copper sample, and for a defect concentrated sample. Copper has a face centered cubic atomic structure, which can be seen in figure 3. The pure copper model is an atomic super cell with dimensions of 4x4x4 atoms, or three cubic structures in each dimension. The model contains 64 total atoms, and is subject to periodic boundaries. The defected copper is model is equivalent, except one of the 64 atoms is removed, simulating a very high defect density. A plot of the bulk copper super-cell's electron wave function can be seen in figure 4. Additionally, the input file for the bulk super-cell is included in the appendix as a sample.

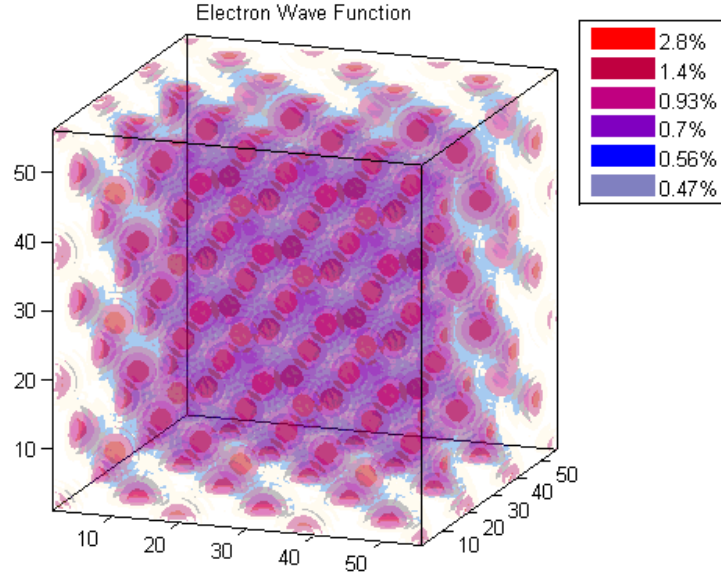


*Fig 3: Electron wave function of a bulk copper super cell. The iso-levels are labeled as percentages of the highest point density plotted.*

## 3.2 Computational Results

The copper structure with a vacancy is simulated to typify defect rich copper samples; and copper structure without vacancies is simulated to model the pure, or bulk, copper that can be achieved through annealing. The difference between the two systems is seen in the final positron density wave function. Since the cross section for particle annihilation depends on the overlap of positron and electron densities, the positron density (specifically the location of its concentration) can be indicative of the probability for valence or core annihilation. The ratio of positron density found near core electrons, compared to valence electrons, varies depending on the atomic structure and defect density. Specifically, the existence of defects in the atomic structure reduces overlap in the core states, and increases overlap in the valence states.

As seen in figure 5, the positron density function for a bulk copper sample, depicts two concentrations, indicating the positrons likely locations. Even in a bulk copper

structure, certain locations are preferable to the positron based on the coulomb and electron magnetic forces. Assuming electron densities are also high in these concentrations, these areas have the highest probability of positron-electron annihilation. The bulk model's positron density concentrates at two spots near its incident location, but shows a minor amount of diffusion that allows for a certain amount of core overlap.

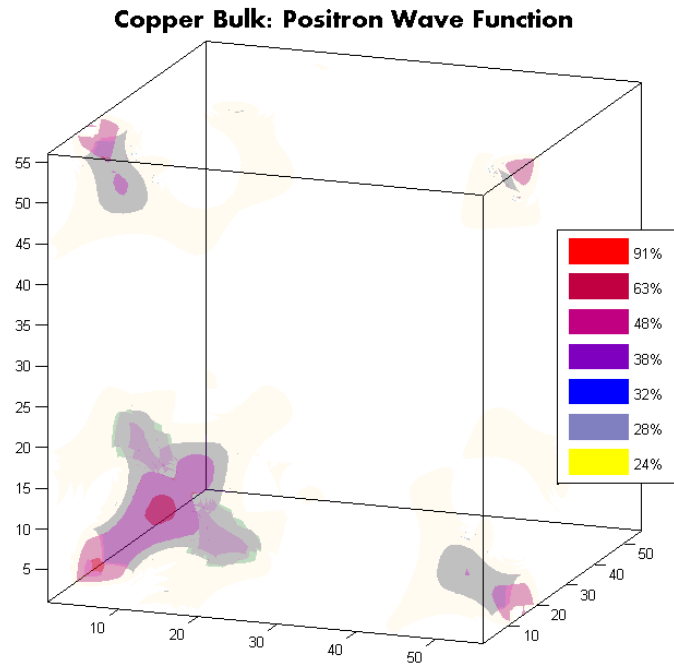


*Fig 4: Calculated positron density wave function for a bulk copper sample. Iso-levels are labeled as percentages of the highest point of density in the plot.*

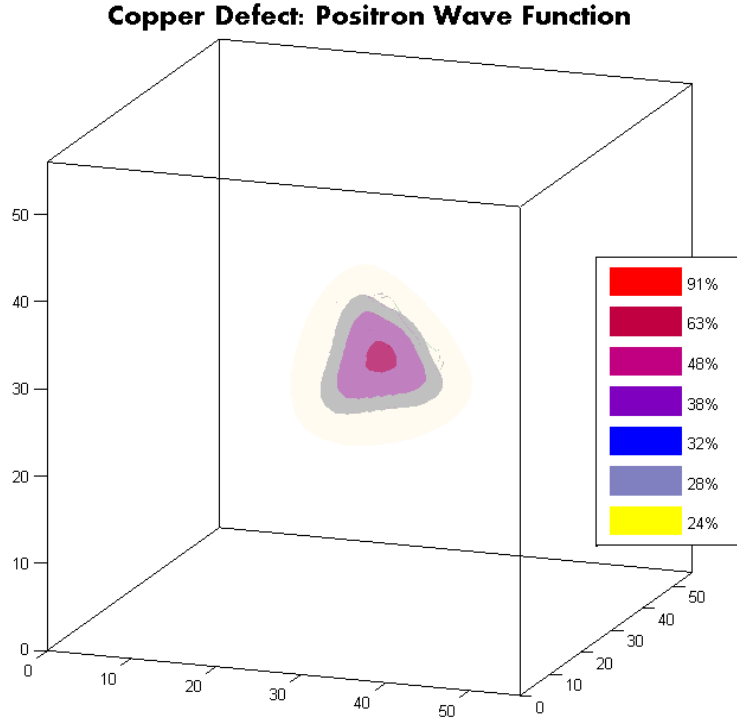


*Fig 5: Calculated positron density wave function for a defect rich copper sample. Iso-levels are labeled as percentages of the highest point of density in the plot.*

In the copper system formed with a vacancy defect, the positron function behaves differently, as depicted in figure 6. The defect is a missing atom in the structure, near the center of the cubic super-cell; and creates a preferable low potential for the positron. The positron function, in this case, shows a strong tendency to be located at the vacancy. It is noteworthy that the vacancy contains a greater density of valence electrons than core electrons.

The calculated momentum distributions from these models are even more important, because they provide statistical and comparable data. Using a line shape parameter, the distributions of the two models can be compared to each other, and other data. The defect free, or bulk, copper model provides a wider momentum peak at zero. This wide peak indicates more annihilations with high momentum, or core level, electrons. The defect-rich, or vacancy, model shows a sharper peak, indicating more low momentum, or valence, annihilations.

In figure 7, plots of the momentum distributions of the two systems are shown adjacently. The distributions are first shown in the decomposed form(separated into each electron shell), and then in a summed form. The vacancy system shows increased prevalence of valence electron state annihilations, which is the largest curve. Also in figure 7, the ratio of the vacancy to the bulk distributions is plotted. The declining ratio shows that the vacancy system has the larger portion of low momentum annihilations, but the bulk system quickly becomes larger at even slightly higher momentums.

In order to calculate a line shape, or curve parameter, consistent energy bounds must be chosen. A study of the decomposed momentum distribution of the bulk system suggests energy bounds, which may be more informative than the standard method when applied to copper structures. In figure 7, a plot of the ratio of core to valence distributions from the bulk model illustrates the momentum energies where core annihilations are most prominent. Choosing bounds that isolate these areas of prominence may result in preferable parameters, more sensitive to core versus valence annihilations.

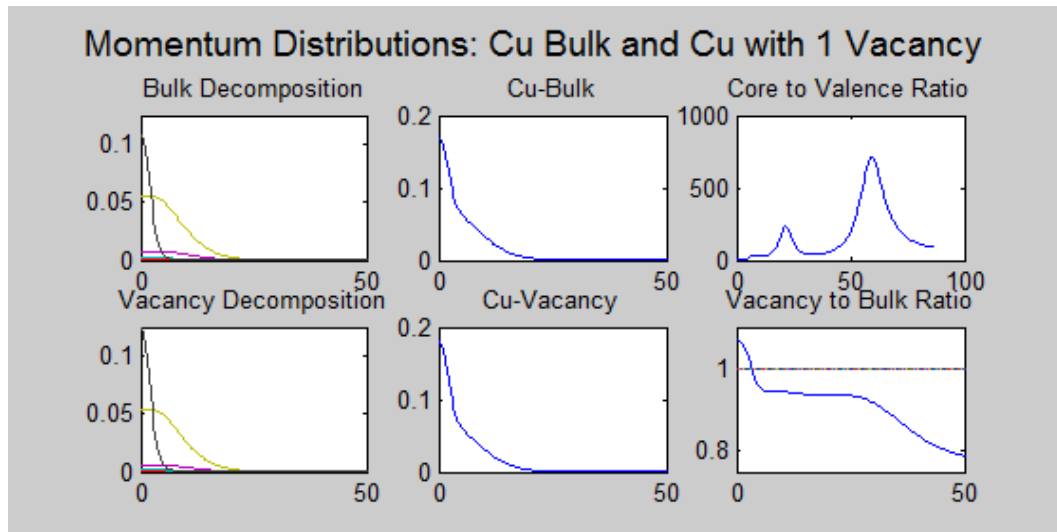


Fig 6: Simulation results of bulk(defect free) and vacancy(defect rich) systems. Momentum is display on the x-axis in units of  $10^{-3} m_0 c$ .



This thesis uses a W parameter (that is associated with high energy, core electron, annihilations) with bounds from 21.5 to 25.2  $10^{-3}m_0c$ ; and an S parameter (associated with low energy, valence electron annihilations) with bounds from 0 to 2.55  $10^{-3}m_0c$ . Finally a standard curve parameter is determined by setting bounds for the bulk copper sample that contain approximately half the peak's total counts. This allows other systems to be easily compared against the bulk system. Based on the collected data for a bulk copper system, the most appropriate bounds for the standard curve parameter are 0 to 3.28  $10^{-3}m_0c$ .

The parameters are calculated by finding the ratio of counts contained in the energy bounds over the total counts contained in the full peak. Table 3 displays all the calculated line shape parameters for the two models, as well as the bounds used for each parameter, and the average momentum of annihilating pairs. The vacancy system shows a higher curve parameter (.530) then the bulk system(.511). This means a higher ratio of annihilation counts occur within the low momentum bounds. More so, the vacancy system shows a higher S parameter, and lower W parameter. These values agree with theory, demonstrating that defects cause sharper spectroscopy energy peaks.

*Table 3: Standard, S, and W line shape parameters for simulation results. Threshold energy bounds and Ave. momentum is given in units of  $10^{-3}m_0c$ .*

	Curve Parameter	S-Low Parameter	W-High Parameter	Ave. Momentum
Cu Bulk	.511	0.425	5.64e-005	0.0601
Cu Vacancy	.53	0.45	4.39e-005	0.0577
Threshold	3.28	2.55	21.5 to 25.2	

# **Chapter 4**

## **Agreement with Experiment**

### **4.1 Experimental Method**

This thesis compares achieved computational data of copper models to experimental data, collected by Doppler spectroscopy on copper samples of varying defect density. The members of the BYU-I physics department performed the experimentation, using a single sensor positron spectroscopy method. One tested copper sample is annealed, and corresponds to the bulk copper computational model. Several more copper samples are implanted with increasing amounts of defects, through abrasion with sand paper of increasing grit intensity.

## 4.2 Comparison of Data

The momentum distributions of the computational models are used to calculate the energy distribution that would be observed in Doppler spectroscopy. For the defect free cases, which are the bulk model and annealed copper experiment, one half of the energy distributions are plotted together in fig.8 for comparison. The computational model shows a sharper center than experimental results, but also shows a more gradual drop at the edges. While the curves are similar, the discrepancy reveals fundamental differences between the computational and experimental methods. The causes for these different shapes is considered in another section.

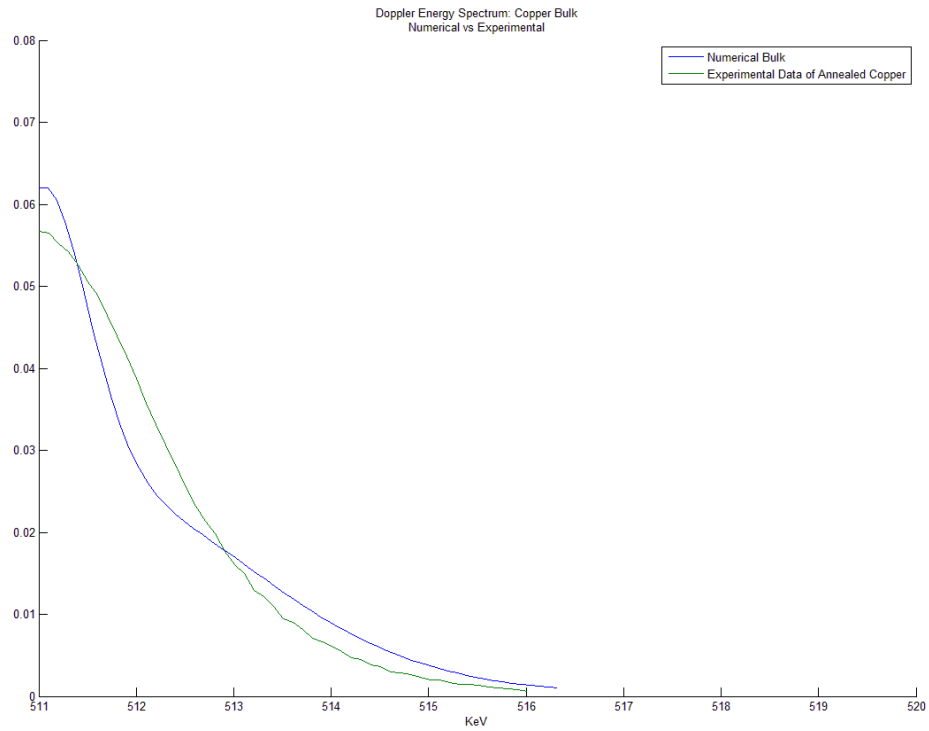


Fig 7: Comparison between a computational and experimental energy distribution.

In contrast to the shape of the energy distributions, the calculated line-shape parameters show agreement between the two methods. Fig. 9 plots a series of curve parameters calculated from the experimental and computational data. Bold circles indicate computational results; similarity between methods, in the effect of defect concentration on S parameters, can easily be seen. The two computational results follow as expected, when compared to the annealed and highest defect density experimental samples.

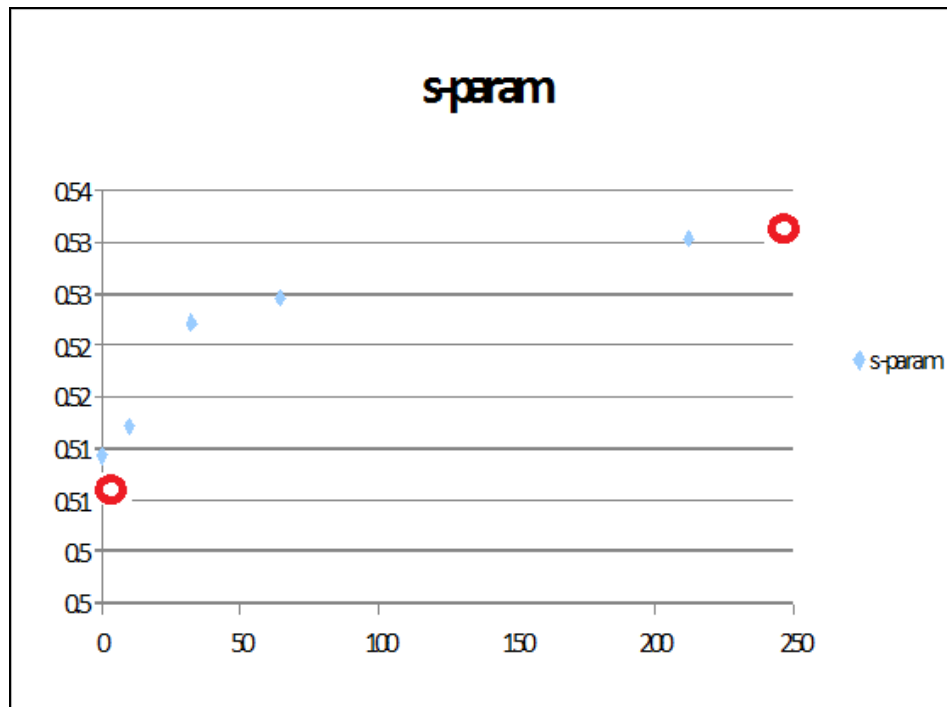


Fig 8: S parameters of varying defect densities. Computational results indicated with

### 4.3 Discrepancies

Even though the computational model provides similar line shape parameters to experiment, the exact shape of the curves indicates a difference between the two methods of data collection. It is most likely, that annihilation events are being simulated properly, but factors that affect experimental observations are not being accounted for.

One major factor that may account for the discrepancy is background noise. A large amount of background photons, which are not produced from positron-electron annihilation, are emitted during spectroscopy. This background is uneven and can dilute or skew the energy distribution; an example is shown in figure 10. The single sensor system used to collect the experimental data is more susceptible to background noise than a possible two sensor, coincidence detection, setup.

The precession of the sensor, and resolution of the experimental setup might also cause the observed differences. To better compare the two methods, one could take into account the accuracy of sensor and dilute the computational data; thus, imitating the limitations of experimental observation.

# Chapter 5

## Ending

The simulated computational models of positron spectroscopy in copper show that defect-rich atomic structures result in a higher line shape parameter. This agrees with theory; and more so, the calculated parameter values show agreement with experimental results for defect-free and defect-rich copper samples.

The exact energy distributions show some discrepancy between the two methods. Further research, to resolve this difference, would increase confidence in the computational model and methods. This would be the best way to further the research conducted in this thesis. As a whole, the computational simulations show a strong agreement to experiment and theory. The overall success of the simulations justifies atomic superposition and density functional theory as accurate and useful methods of computationally modeling positron spectroscopy in solids.

# Bibliography

[1] Grafutin, Viktor I., and Evgenii P. Prokop'ev. "Positron Annihilation Spectroscopy in Materials Structure Studies." *Physics-Uspekhi* 45.1 (2002): 59-74. Print.

[2] Sholl, David S., and Janice A. Steckel. *Density Functional Theory: A Practical Introduction*. Hoboken, NJ: Wiley, 2009. Print.

[3] Laboratory of Physics Helsinki University of Technology, comp. "Doppler: A Program to Model Positron States and Annihilation in Solids." (2003).

# Appendix A

## Samples

Example input file used for bulk copper model:

1 0.FALSE..TRUE..FALSE.	1 34 1.25 0.25 0.25 0.
.FALSE..FALSE.	1 35 0.25 1.25 0.25 0.
0.22 1 1 0.01	1 36 1.25 1.25 0.25 0.
.FALSE.	1 37 0.25 0.25 1.25 0.
64	1 38 1.25 0.25 1.25 0.
Cu	1 39 0.25 1.25 1.25 0.
7	1 40 1.25 1.25 1.25 0.
6.8219 0.5 1.0	1 41 0.75 0.75 0.25 0.
56 56 56 12. 1d-12	1 42 1.75 0.75 0.25 0.
999999999999. 1.0 1.	1 43 0.75 1.75 0.25 0.
2. 0. 0.	1 44 1.75 1.75 0.25 0.
0. 2. 0.	1 45 0.75 0.75 1.25 0.
0. 0. 2.	1 46 1.75 0.75 1.25 0.
1 1 0 0 0 0.	1 47 0.75 1.75 1.25 0.
1 2 1 0 0 0.	1 48 1.75 1.75 1.25 0.
1 3 0 1 0 0.	1 49 0.75 0.25 0.75 0.
1 4 1 1 0 0.	1 50 1.75 0.25 0.75 0.
1 5 0 0 1 0.	1 51 0.75 1.25 0.75 0.
1 6 1 0 1 0.	1 52 1.75 1.25 0.75 0.
1 7 0 1 1 0.	1 53 0.75 0.25 1.75 0.
1 8 1.25 1.75 1.75 0.	1 54 1.75 0.25 1.75 0.
1 9 0.5 0.5 0 0.	1 55 0.75 1.25 1.75 0.
1 10 1.5 0.5 0 0.	1 56 1.75 1.25 1.75 0.
1 11 0.5 1.5 0 0.	1 57 0.25 0.75 0.75 0.
1 12 1.5 1.5 0 0.	1 58 1.25 0.75 0.75 0.
1 13 0.5 0.5 1 0.	1 59 0.25 1.75 0.75 0.
1 14 1.5 0.5 1 0.	1 60 1.25 1.75 0.75 0.
1 15 0.5 1.5 1 0.	1 61 0.25 0.75 1.75 0.
1 16 1.5 1.5 1 0.	1 62 1.25 0.75 1.75 0.
1 17 0.5 0 0.5 0.	1 63 0.25 1.75 1.75 0.
1 18 1.5 0 0.5 0.	1 64 1 1 1 0.
1 19 0.5 1 0.5 0.	1.0 5000
1 20 1.5 1 0.5 0.	6
1 21 0.5 0 1.5 0.	1 1 1
1 22 1.5 0 1.5 0.	1
1 23 0.5 1 1.5 0.	-1 -1 -2
1 24 1.5 1 1.5 0.	1.FALSE..FALSE..FALSE..FALSE.
1 25 0 0.5 0.5 0.	s
1 26 1 0.5 0.5 0.	60 1e-6 1 7 0400
1 27 0 1.5 0.5 0.	3
1 28 1 1.5 0.5 0.	2 4 8
1 29 0 0.5 1.5 0.	1
1 30 1 0.5 1.5 0.	1
1 30 1 0.5 1.5 0.	1
1 31 0 1.5 1.5 0.	2
1 32 1 1.5 1.5 0.	1
1 33 0.25 0.25 0.25 0.	3
	.TRUE